Proc. Indian Acad. Sci. (Chem. Sci.), Vol. 106, No. 2, April 1994, pp. 229–249.

A dynamical study of the principle of maximum hardness

P K CHATTARAJ* and S NATH
Department of Chemistry, Indian Institute of Technology, Kharagpur 721 302, India

Abstract. Temporal evolution of local and global hardness during an ion-atom collision process has been studied within a quantum fluid density functional framework. A dynamical variant of the maximum hardness principle has been found to be operative. Entropy maximises in the encounter regime. Time dependence of density and its laplacian provides important insights into the collision process *vis-a-vis* the hardness maximisation.

Keywords. Maximum hardness principle; time dependence; entropy; laplacian of density.

1. Introduction

Hardness (η) (Parr and Pearson 1983) and chemical potential (μ) (Parr *et al* 1978) are two important concepts in chemistry. Within density functional theory (DFT) they are defined as (Parr *et al* 1978; Parr and Pearson 1983; Sen and Jorgensen 1987; Pearson 1988, 1990; Chattaraj 1992b; Chattaraj and Parr 1993; Sen and Mingos 1993)

$$\eta = \frac{1}{2}\left[\frac{\partial \mu}{\partial N}\right]_{v(\mathbf{r})} = \frac{1}{2}\left[\frac{\partial^2 E}{\partial N^2}\right]_{v(\mathbf{r})}, \tag{1}$$

and

$$\mu = \left[\frac{\partial E}{\partial N}\right]_{v(\mathbf{r})}, \tag{2}$$

where E and $v(\mathbf{r})$ are electronic energy and external potential of an N-electron system respectively. Definitions (1) and (2) remain unaltered, within the Born–Oppenheimer approximation, in case total energy is used in place of electronic energy. Assuming validity of Koopmans' theorem for closed shell molecules, η and μ can be written as (Pearson 1987)

$$\eta = (1/2)(\varepsilon_{\mathrm{LUMO}} - \varepsilon_{\mathrm{HOMO}}), \tag{3}$$

$$\mu = (1/2)(\varepsilon_{\mathrm{HOMO}} + \varepsilon_{\mathrm{LUMO}}), \tag{4}$$

where $\varepsilon_{\mathrm{HOMO}}$ and $\varepsilon_{\mathrm{LUMO}}$ denote energies of HOMO and LUMO. Reciprocal of hardness is softness (Yang and Parr 1985) given by

$$\Sigma = \frac{1}{2\eta} = \left[\frac{\partial N}{\partial \mu}\right]_{v(\mathbf{r})}. \tag{5}$$

*For correspondence

It was found that the stability of a chemical species can be associated with its hardness. Pearson (1987) postulated the principle of maximum hardness as "there seems to be a rule of nature that molecules arrange themselves so as to be as hard as possible". Later Zhou *et al* (1988) and Zhou and Parr (1989, 1990) established the connection between aromaticity/stability and hardness which has been associated with half of the HOMO–LUMO gap. Zhou and Parr (1990) discussed the maximum hardness principle (MHP) within the Hückel molecular orbital (HMO) theory. A formal proof of maximum hardness (minimum softness) principle has been provided by Parr and Chattaraj (1991) using the fluctuation–dissipation theorem of statistical mechanics. They have considered the electronic system of interest as a member of a grand canonical ensemble with bath parameters $\mu, v(\mathbf{r})$ and temperature, θ. It has been shown that any nearby nonequilibrium state of the system will evolve towards the equilibrium state with maximum hardness provided the bath parameters do not change. The applicability of statistical mechanics to a many-electron chemical system has been assumed in the proof. Various studies confirm the validity of such an assumption (Parr and Yang 1989). An alternate proof of MHP has been provided very recently by Parr and Gazquez (1993) through the construction of a new ground state hardness functional. The proof of MHP (Parr and Chattaraj 1991) has been supported by several subsequent papers. Pearson and Palke (1992) calculated η and μ from (3) and (4) for vibrational modes of NH_3 and C_2H_6 molecules using *ab initio* molecular orbital (MO) theory and found that in asymmetric vibration modes in which μ and $v(\mathbf{r})$ remain constant for small change, η is maximum for the equilibrium geometry. But for symmetric vibration mode, in which neither μ nor $v(\mathbf{r})$ is constant, variation of η is monotonic. Same conclusion has been reached by Chattaraj *et al* (1993) when vibrational modes for several molecules belonging to C_{2v}, C_{3v}, $C_{\infty v}$ and $D_{\infty h}$ point groups were considered. The importance of nuclear repulsion energy (v_{nn}) in determining a state of maximum hardness has been discussed by Parr and Gazquez (1993). They have shown that for a state with maximum hardness, electronic energy (E) and nuclear repulsion energy reach their respective extremum values. It has been found that for asymmetric vibrations, v_{nn} remains more or less constant, while it changes monotonically for symmetric vibrations. The fact that E reaches its minimum at the equilibrium state in case of asymmetric vibrations but changes monotonically in the symmetric mode explains why hardness reaches its maximum value at equilibrium in case of asymmetric vibrations only. It has been found by MNDO calculations that thermodynamically favourable exchange reactions proceed in a direction which produces hardest possible products (Datta 1992a). The same conclusion has been reached for exchange reactions where anomeric effect is operative (Hati and Datta 1992). It was shown both in MNDO (Datta 1992b) and *ab initio* SCF (Chattaraj *et al* 1993) level calculations that the transition state of a reaction is associated with minimum hardness which is in agreement with MHP. It has been found that MHP is useful in detecting the most stable isomer of a chemical compound. Work carried out on Si_4 clusters (Galvan *et al* 1993), Si_2H_2 and alkali metal carbonyl cations (Chattaraj *et al* 1993) shows that the isomer having the least energy has the highest value of hardness. In these cases MHP has been found to be valid even if the conditions of constant μ and $v(\mathbf{r})$ are not satisfied. Relatively more stable lithium clusters comprising the 'magic number' of atoms and exhibiting intense mass spectral peaks are found to have relatively larger hardness values (Harbola 1992). In this study μ has a constant value but $v(\mathbf{r})$ changes with the number of electrons. Impurity

segregation at grain boundaries has also been analysed (Dal Pino *et al* 1993) in the light of MHP. Chattaraj and coworkers have studied the implications of MHP in static (Chattaraj *et al* 1993; Chattaraj and Schleyer 1994; Nath *et al* 1994) and dynamic (Chattaraj and Nath 1994b) situations.

It has been suggested (Berkowitz *et al* 1985; Ghosh and Berkowitz 1985) that hardness of a chemical species at equilibrium is not constant over space although the chemical potential is. The local variant of hardness has been found to account for chemical reactivity. By studying the profiles of local quantities like local hardness (Berkowitz *et al* 1985; Ghosh and Berkowitz 1985), local softness (Yang and Parr 1985) and Fukui function (Parr and Yang 1982) which are expressed below, one can predict the type of attack (electrophilic, nucleophilic or radical), the site for attack and the orientation of attacking molecule. Local hardness is given by (Berkowitz *et al* 1985)

$$\eta(\mathbf{r}) = (1/2)\left[\frac{\delta\mu}{\delta\rho}\right]_{v(\mathbf{r})} \tag{6}$$

or as the following density functional (Berkowitz *et al* 1985; Ghosh and Berkowitz 1985)

$$\eta(\mathbf{r}) = \frac{1}{2N}\int \frac{\delta^2 F[\rho]}{\delta\rho(\mathbf{r})\,\delta\rho(\mathbf{r}')}\rho(\mathbf{r}')\mathrm{d}\mathbf{r}', \tag{7}$$

where $F[\rho]$ is the Hohenberg–Kohn (HK) universal functional consisting of kinetic energy (KE), electron–electron repulsion energy and exchange correlation energy functionals. Expressions for Fukui function $f(\mathbf{r})$ (Parr and Yang 1982) and local softness $\sigma(\mathbf{r})$ (Yang and Parr 1985) are respectively as follows,

$$f(\mathbf{r}) = \left[\frac{\partial\rho}{\partial N}\right]_{v(\mathbf{r})}, \tag{8}$$

$$\sigma(\mathbf{r}) = \left[\frac{\partial\rho}{\partial\mu}\right]_{v(\mathbf{r})}. \tag{9}$$

Local hardness and softness integrates to corresponding global quantities as

$$\eta = \int f(\mathbf{r})\eta(\mathbf{r})\,\mathrm{d}\mathbf{r}, \tag{10}$$

$$\Sigma = \int \sigma(\mathbf{r})\,\mathrm{d}\mathbf{r}. \tag{11}$$

Although MHP has been found to be valid in a number of situations a detailed dynamical study of it is still awaited. In the present work, we have studied the time evolution of global as well as local hardness in a chemical reaction modelled as a collision process between a proton and a nitrogen atom. We also have studied the time evolution of electron density, $\rho(\mathbf{r}, t)$, effective potential, $v_{\mathrm{eff}}(\mathbf{r}, t)$, and current density, $|\mathbf{j}(\mathbf{r}, t)|$ to follow the time-dependent process. In this context, we have tried to understand the prognosis of Bader *et al* (1984) that the Laplacian of density ($\nabla^2\rho$) could be used to predict the hard–soft behaviour of an atom or a molecule. For this

purpose we have compared the spatial profiles of $-\nabla^2\rho$ and $\eta(\mathbf{r})$ at different time steps. In the ion–atom collision process, we have also studied the time dependence of entropy and surprisal which give information of a dynamic process. In dynamic situations, entropy reaches a maximum which is a consequence of Jaynes' (1963) maximum entropy principle (MEP). In the present work, entropy has been taken from Deb and Chattaraj (1989) who defined the entropy density functional for a system of N noninteracting particles moving under an effective potential field.

The main objective of this study is to understand how local and global hardness as well as entropy vary with time ("along the reaction path") in order to have a better understanding of the maximum hardness and the maximum entropy principles in a dynamical situation. Collision between a proton and a nitrogen atom has been taken as a test case and has been studied within a quantum fluid density functional (QFDF) framework whose basic formalism was developed by Deb and Chattaraj (1989). The QFDF theory has been applied to solve various time dependent problems, viz., H^+–Ne collision problem using an alternating direction implicit method (Deb and Chattaraj 1989) and the problems of an He atom colliding with H^+ (Deb *et al* 1991) as well as interacting with an intense laser field (Chattaraj 1992a) using a leapfrog finite difference scheme. Note that the numerical algorithms developed so far to solve time-dependent problems within QFDF theory would allow us to study only H^+-atom collision problems. Studies on ion (other than H^+)–atom, atom–atom, atom–molecule, molecule–molecule and gas–surface collisions require different algorithms which can take care of electronic/vibrational/rotational states of the projectile and vibrational/rotational states of the target. It is for the first time that we are solving a collision problem within QFDF theory involving an open-shell system and calculating the time evolution of local and global hardness as well as entropy of that system by writing them as density functionals. We have studied the H^+–N collision because of the theoretical (Liu and Verhaegen 1970) and experimental (Colin and Douglas 1968) importance of NH^+, which is a stable molecule of chemical and astrophysical interest (Liu and Verhaegen 1970; Huber and Herzberg 1979; Baeck and Lee 1990), with a dissociation energy value of 3·39 ev. It is worth noting that this dissociation energy corresponds to $N(^4S)$ and H^+ whereas the dissociation products for the $^2\Pi$ ground state are $N^+(^3P) + H(^2S)$. It suggests that collision of $N(^4S)$ and H^+ may lead to the formation of NH^+ in the electronically excited $^4\Sigma^-$ state.

2. Methodology

The key equation in QFDF theory is a generalised nonlinear Schrödinger equation (GNLSE) (Deb and Chattaraj 1988, 1989; Deb *et al* 1991; Chattaraj 1992a) given by

$$[-1/2\,\nabla^2 + v_{\text{eff}}(\mathbf{r},t)]\,\phi(\mathbf{r},t) = i\frac{\partial\phi(\mathbf{r},t)}{\partial t}. \tag{12}$$

This equation has been derived from the following QFD equations involving $\rho(\mathbf{r},t)$ and a velocity potential $\chi(\mathbf{r},t)$, viz.,

$$\frac{\partial\rho}{\partial t} + \nabla\cdot(\rho\nabla\chi) = 0, \tag{13}$$

$$\frac{\partial\chi}{\partial t}+1/2(\nabla\chi)^2+\frac{\delta G[\rho]}{\delta\rho}+\int\frac{\rho(\mathbf{r}',t)}{|\mathbf{r}-\mathbf{r}'|}\mathrm{d}\mathbf{r}'-\frac{Z}{r}+v_{ext}(\mathbf{r},t)\equiv 0, \tag{14}$$

using polar form of wavefunction written as

$$\phi(\mathbf{r},t)=\rho^{1/2}\exp(i\chi). \tag{15}$$

In (14) $G[\rho]$ consists of kinetic and exchange-correlation energy functionals, i.e.

$$G[\rho]=T[\rho]+E_{xc}[\rho], \tag{16}$$

where

$$E_{xc}[\rho]=-\int C_x\rho^{4/3}\mathrm{d}\mathbf{r}-\int\frac{\rho}{9{\cdot}81+21{\cdot}437\rho^{-1/3}}\mathrm{d}\mathbf{r}, \tag{17}$$

and

$$C_x=(3/4\pi)(3\pi^2)^{1/3}.$$

$T[\rho]$ can be divided into atomic and molecular parts (Deb and Chattaraj 1989) as

$$T[\rho]=T_{\mathrm{at}}[\rho]+T_{\mathrm{mol}}[\rho] \tag{18}$$

where $T_{\mathrm{mol}}[\rho]$ has been expressed as

$$T_{\mathrm{mol}}[\rho]=\int\frac{f(R,N)}{N}\rho\,\mathrm{d}\mathbf{r}, \tag{19}$$

and

$$f(R,N)=(1/R^{12})(N/10)^{14}R^2\exp(-0{\cdot}8R). \tag{20}$$

In (19) R is the internuclear distance. The atomic part of the KE functional is given by

$$T_{\mathrm{at}}[\rho]=C_K\int\rho^{5/3}\mathrm{d}\mathbf{r}+\frac{1}{8}\int\frac{\nabla\rho\cdot\nabla\rho}{\rho}\mathrm{d}\mathbf{r}+a(N)\int\frac{\mathbf{r}\cdot\nabla\rho}{r^2}\mathrm{d}\mathbf{r} \tag{21}$$

where $a(N)$ is an N-dependent constant expressed as (Ghosh and Balbas 1985)

$$a(N)=a_0+a_1N^{-1/3}+a_2N^{-2/3},$$

and

$$C_K=(3/10)(3\pi^2)^{2/3}.$$

In (12) v_{eff} is given by

$$v_{\mathrm{eff}}(\mathbf{r},t)=\frac{5}{3}C_K\rho^{2/3}-\frac{a(N)}{r^2}+\frac{f(R,N)}{N}+\frac{\delta E_{xc}}{\delta\rho}+\int\frac{\rho(\mathbf{r}',t)}{|\mathbf{r}-\mathbf{r}'|}\mathrm{d}\mathbf{r}'-\frac{Z}{r}+v_{\mathrm{ext}}(\mathbf{r},t). \tag{22}$$

In (22) $v_{\mathrm{ext}}(\mathbf{r},t)$ is the time-dependent external potential which can be written as,

$$v_{\mathrm{ext}}(\mathbf{r},t)=-\frac{1}{|\mathbf{R}(t)-\mathbf{r}|}, \tag{23}$$

where $\mathbf{R}(t)$ is the classical trajectory on which two nuclei move. Assuming that the proton is approaching the nitrogen nucleus in a straight line with velocity v_p, the

expression for $\mathbf{R}(t)$ becomes

$$\mathbf{R}(t) = [b^2 + z^2(t)],$$
$$z(t) = [z(0) - v_p t], \tag{24}$$

where b is the impact parameter and $z(t)$ is the z coordinate of the proton at time t in a rotating coordinate frame. Cylindrical symmetry of the system permits integration over the azimuthal angle analytically.

To calculate time-dependent density, $\rho(\mathbf{r}, t)$, (12) has been solved at every time step using a leapfrog finite difference scheme. A near Hartree–Fock (HF) density profile of nitrogen atom in the ^{4}S state (Clementi and Roetti 1974) has been used as input at $t = 0$. The numerical solution of (12) has already been discussed at length elsewhere (Deb *et al* 1991; Chattaraj 1992a).

In a TD process, knowledge of current density is essential along with the knowledge of electron density since all properties including time-dependent energy are unique functionals of $\rho(\mathbf{r}, t)$ and $\mathbf{j}(\mathbf{r}, t)$ according to TDDFT (Runge and Gross 1984; Dhara and Ghosh 1987). Current density is expressed as

$$\mathbf{j}(\mathbf{r}, t) = [\phi_{re} \nabla \phi_{im} - \phi_{im} \nabla \phi_{re}] = \rho \nabla \chi. \tag{25}$$

Local hardness has been calculated from (7) using HK functional as

$$F[\rho] = T[\rho] + E_{xc}[\rho] + \frac{1}{2} \int \int \frac{\rho(\mathbf{r}) \rho(\mathbf{r}')}{|\mathbf{r} - \mathbf{r}'|} d\mathbf{r}\, d\mathbf{r}', \tag{26}$$

where the forms for $T[\rho]$ and $E_{xc}[\rho]$ are as given in (18)–(21) and (17) respectively. Time evolution of $\eta(\mathbf{r})$ has been obtained after calculating TD charge density $\rho(\mathbf{r}, t)$ at every time step. Global hardness can be obtained from (10) provided time evolution of $f(\mathbf{r})$ is known. Following Berkowitz *et al* (1985), the expression for Hellmann–Feynman force is written as

$$\int \rho(\mathbf{r})\, dv(\mathbf{r}) d\mathbf{r} = N \int f(\mathbf{r}) dv(\mathbf{r}) d\mathbf{r} - 4N \operatorname{Re} \left\{ \sum_k{}' \frac{\langle \psi_0 | dv | \psi_k \rangle \langle \psi_0 | \eta(\mathbf{r}) | \psi_k \rangle}{E_k - E_0} \right\}. \tag{27}$$

Since the second term in the right hand side of (27) is often small (Berkowitz *et al* 1985) we neglect it to get an approximate form for $f(\mathbf{r})$ as

$$f(\mathbf{r}) = \rho(\mathbf{r})/N, \tag{28}$$

which and consequently the hardness functional obtained from (10) can be improved by incorporating appropriate inhomogeneity corrections in (28). It should be mentioned in this context that a similar approximate form for $f(\mathbf{r})$ has been obtained by Gazquez (1993) considering an uniform charge addition and removal to be natural in a density functional framework. Very recently Parr and Gazquez (1993) have suggested a more general hardness functional.

Taking the expression of $f(\mathbf{r})$ from (28) global hardness becomes

$$\eta(t) = (1/N) \int \eta[\rho(\mathbf{r}, t)]\, \rho(\mathbf{r}, t) d\mathbf{r}. \tag{29}$$

Here, it may be noted that there is some ambiguity in the definition of $\eta(\mathbf{r})$ (Harbola *et al* 1991) since it requires change in $\rho(\mathbf{r})$ at constant $v(\mathbf{r})$ which are interdependent according to the HK theorem (Hohenberg and Kohn 1964). In a time-dependent situation also the invertibility of the map between $\rho(\mathbf{r}, t)$ and $v(\mathbf{r}, t)$ has been established (Runge and Gross 1984; Dhara and Ghosh 1987). Although the unambiguous definition for $\eta(\mathbf{r})$ is that it is equal to global hardness, other definitions for $\eta(\mathbf{r})$ would be useful in specific situations (Harbola *et al* 1991). It is also tacitly assumed that whatever ambiguity is present at $t = 0$, will remain unchanged during time evolution and the qualitative nature of the temporal evolution of local and global hardness will not be disturbed.

Considering an N-electron system as a system of N noninteracting particles moving under the influence of $v_{\text{eff}}(\mathbf{r}, t)$, entropy density is defined using an average density argument as (Deb and Chattaraj 1989),

$$s(\mathbf{r}, t) = (5/2)k\rho - k\rho \ln \rho + (3/2)k\rho \ln\left(\frac{k\theta}{2\pi}\right), \tag{30}$$

where k is the Boltzmann constant and θ is a space–time dependent 'temperature' defined in terms of KE density as,

$$t_s(\mathbf{r}; \rho(\mathbf{r}, t)) = (3/2)\,\rho(\mathbf{r}, t)\,k\theta(\mathbf{r}, t) + (|\mathbf{j}|^2/2\rho). \tag{31}$$

Equation (30) can also be obtained from information theory by writing Shanon entropy for the system involving $\rho(\mathbf{r}, t)$ and maximising it under certain constraints. The global entropy is obtained by integrating (30) over whole space,

$$S = \int s(\mathbf{r}, t)\mathrm{d}\mathbf{r}. \tag{32}$$

Surprisal of the distribution is defined as (Levine and Bernstein 1976; Gadre and Bendale 1985; Chattaraj 1992a),

$$I(\mathbf{r}, t) = -\ln\left[\frac{\rho(\mathbf{r}, t)}{\rho^{\text{HF}}(\mathbf{r}, 0)}\right], \tag{33}$$

where $\rho^{\text{HF}}(\mathbf{r}, 0)$ is the near Hartree–Fock density at $t = 0$.

3. Results and discussion

Spatial profiles of $v_{\text{eff}}, \rho, \mathbf{j}, -\nabla^2\rho, \eta(\mathbf{r}), s$ and I are plotted in cylindrical polar coordinate $(\tilde{\rho}, \tilde{z})$ mesh at different time steps.

Figures 1a–c show the spatial profiles of v_{eff} at $t = 0$, 5, and 15 (all in a.u.). The vertical dimension of v_{eff} is taken from -50 to $+50$. At $t = 0$, the plot of v_{eff} consists of a deep well at the nuclear site ($\tilde{\rho} = 0$, $\tilde{z} = 0$) due to the attractive potential. This infinite trough is surrounded by a valley-like structure. There are small undulations around $\tilde{z} = 0$ and along the increasing $\tilde{\rho}$ axis (figure 1a). At $t = 5$ a.u., besides the attractive region around the nucleus, a high peak of positive potential builds up in front of the deep well, and several small peaks and troughs are formed along the

increasing ρ axis around $z = 0$ (figure 1b). At $t = 15$ a.u. when the proton comes very close to the nitrogen atom, two troughs are formed along the $\tilde{z}$ axis placed symmetrically at the two sides of the central attractive zone (figure 1c). All other features of the v_{eff} plot remain almost similar to that of figure 1b.

Figure 2a shows spatial variation of charge density at $t = 0$. In this figure ρ is found to have a maximum around the origin ($\tilde{\rho} = 0$, $\tilde{z} = 0$) where the attractive potential dominates. In later time steps (figures 2b and c) density accumulates at the nuclear region due to the nonlinear effective potential. At $t = 15$ a.u. the profile of ρ

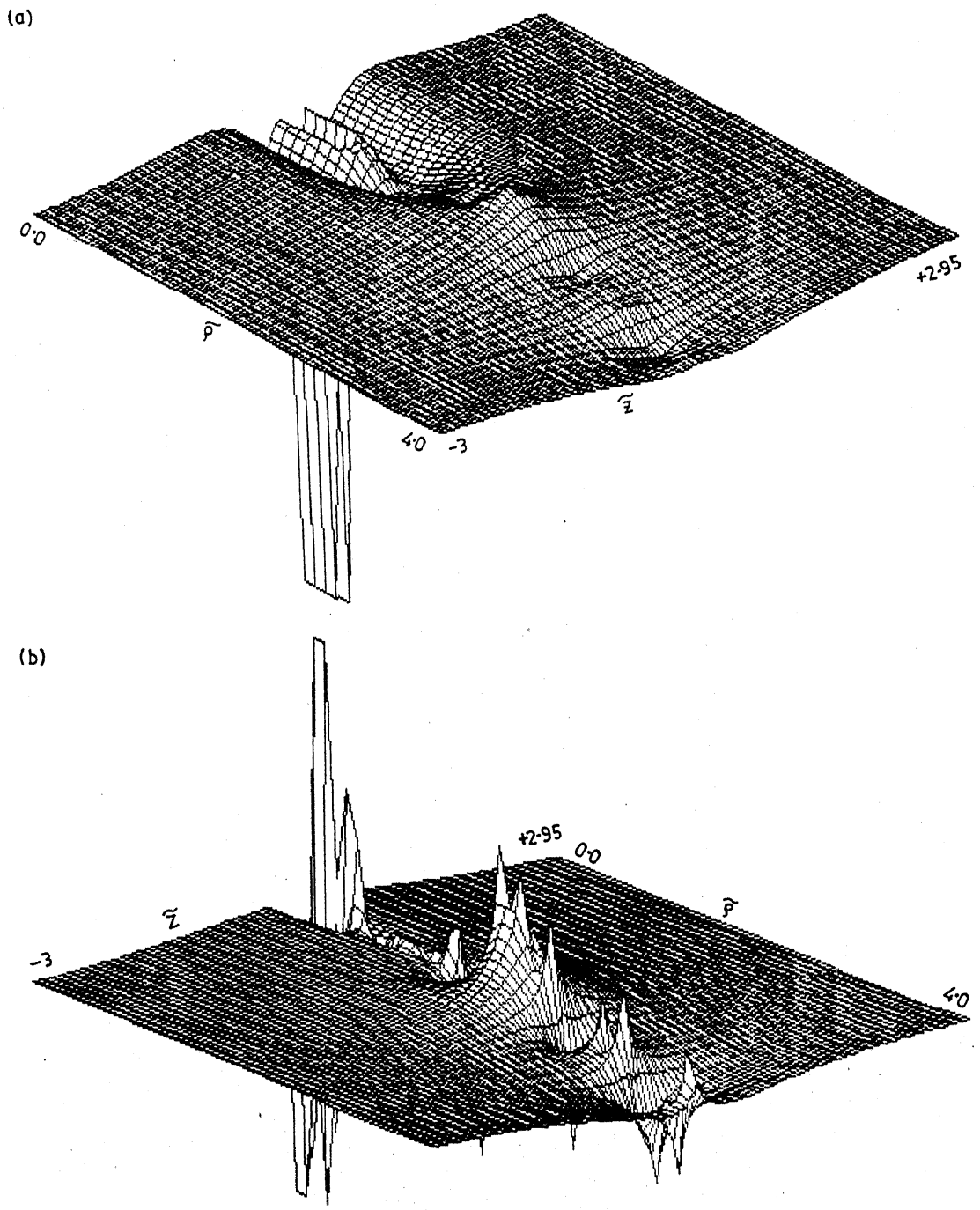

Figure 1. (a) & (b) (Caption on facing page.)

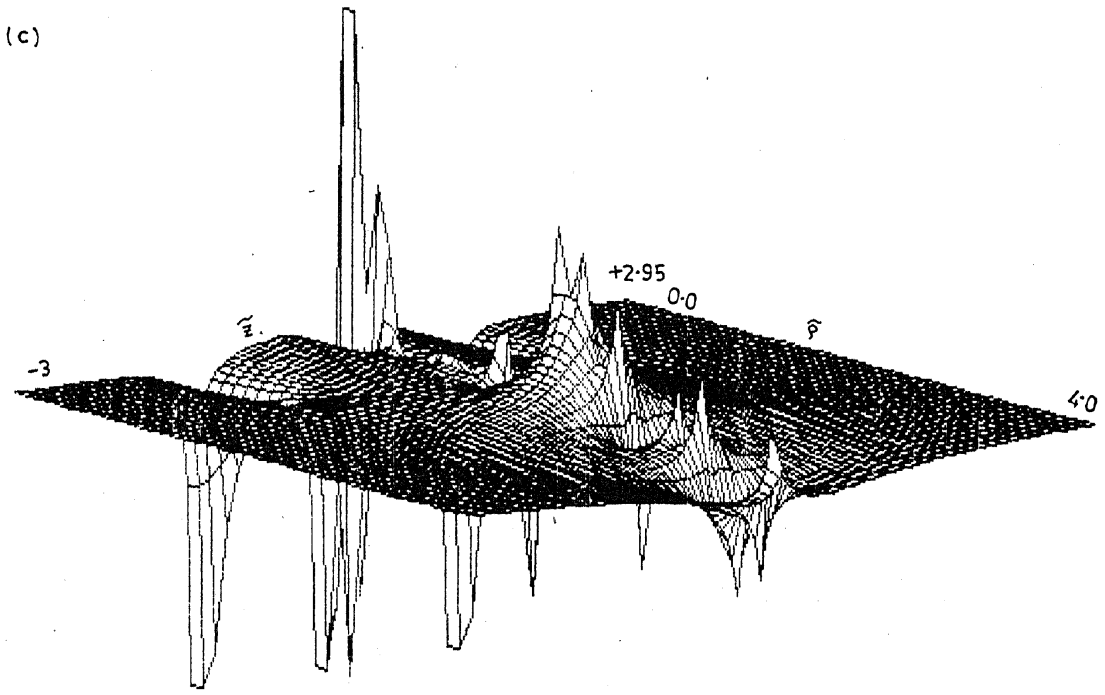

Figure 1. Perspective plots (a.u.) of effective potential (v_{eff}) of nitrogen atom colliding with a proton in cylindrical polar coordinates $(\tilde{\rho}, \tilde{z})$. The basal rectangular mesh designates the $(\tilde{\rho}, \tilde{z})$ plane where $0 \leqslant \tilde{\rho} \leqslant 4$ and $-3 \leqslant \tilde{z} \leqslant 2{\cdot}95$. The nucleus of nitrogen atom is at $(0,0)$. $t = 0{\cdot}0$ (**a**), $5{\cdot}0$ (**b**), $15{\cdot}0$ (**c**).

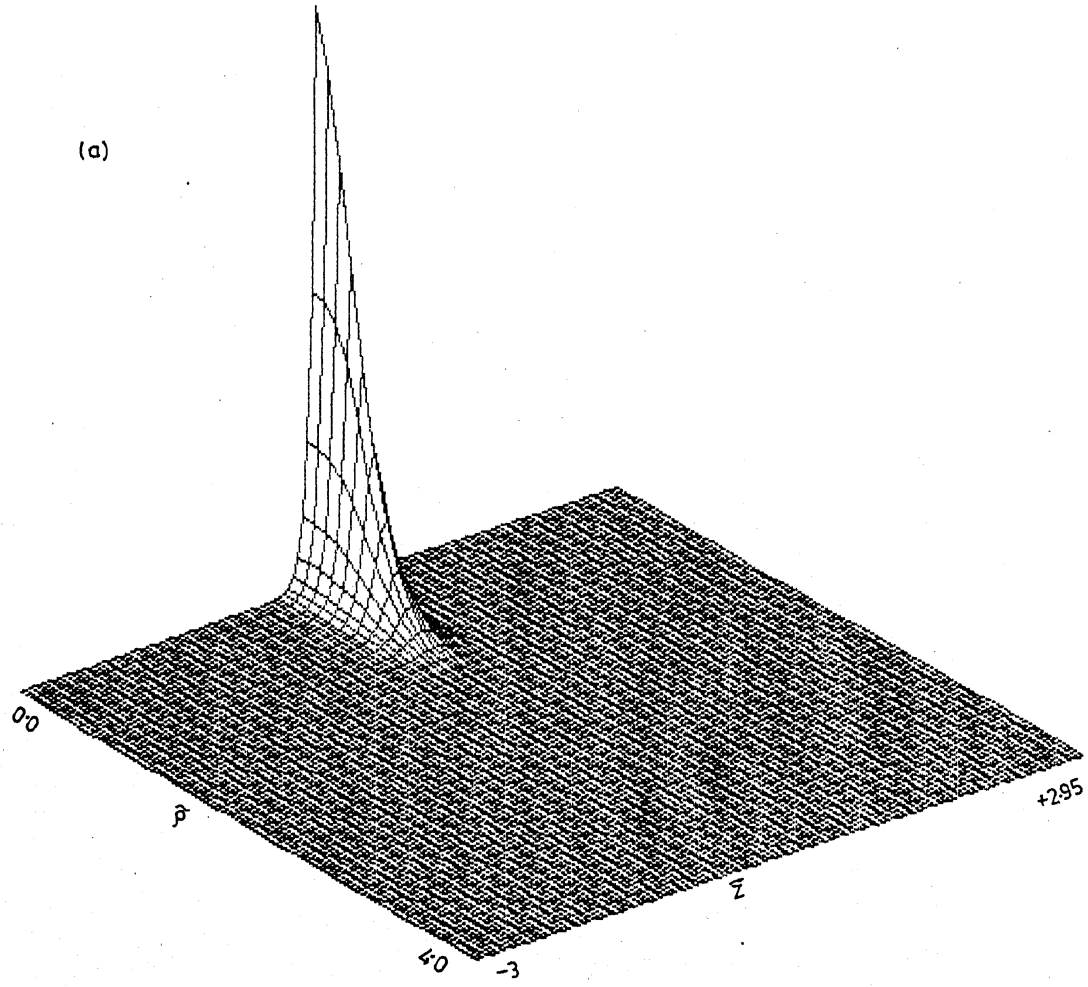

Figure 2. (**a**) (Caption on next page.)

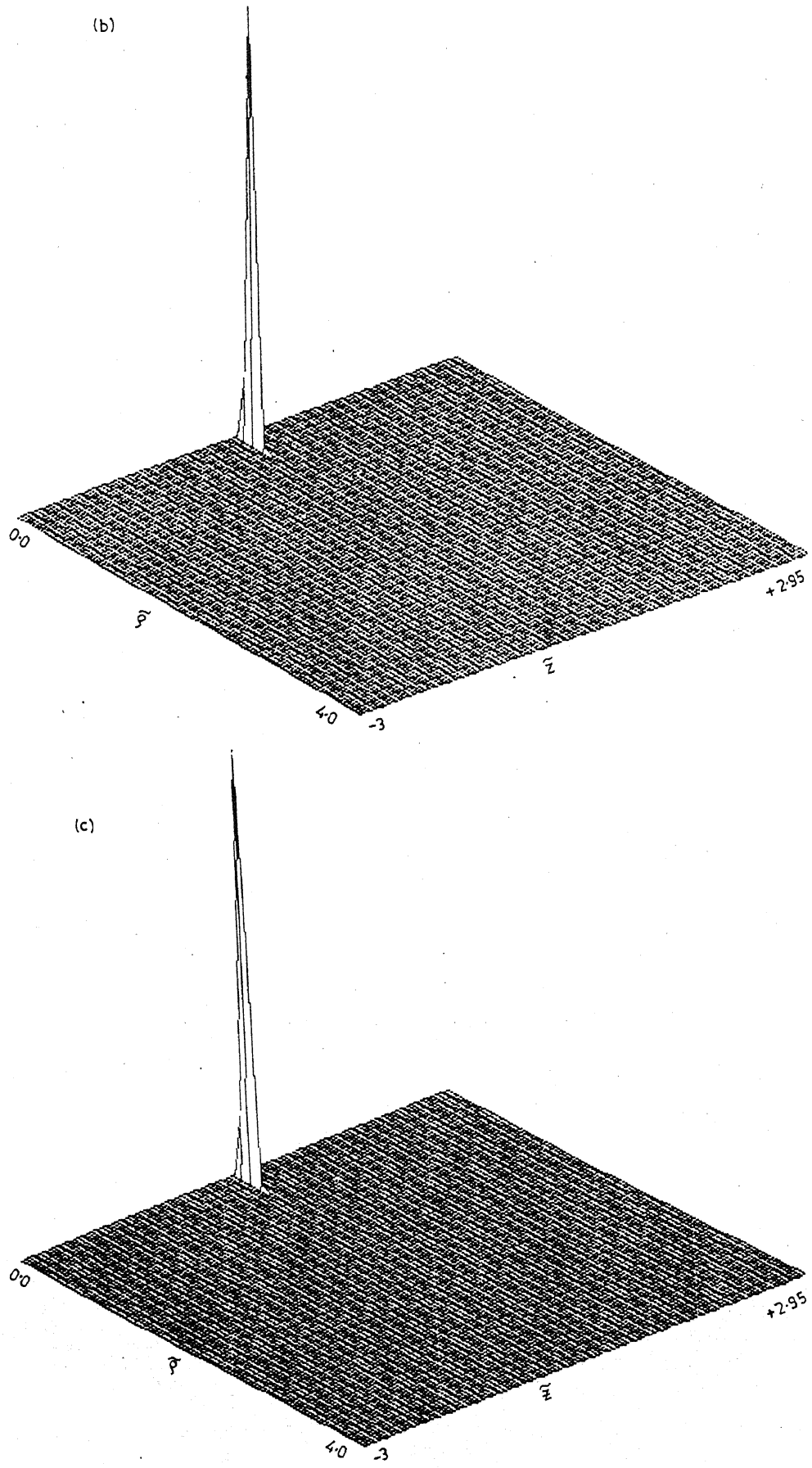

Figure 2. Perspective plots (a.u.) of electron density (ρ) of nitrogen atom colliding with a proton in cylindrical polar coordinates ($\tilde{\rho}, \tilde{z}$). See caption of figure 1 for details. $t = 0{\cdot}0$ (**a**), 5·0 (**b**), 15·0 (**c**).

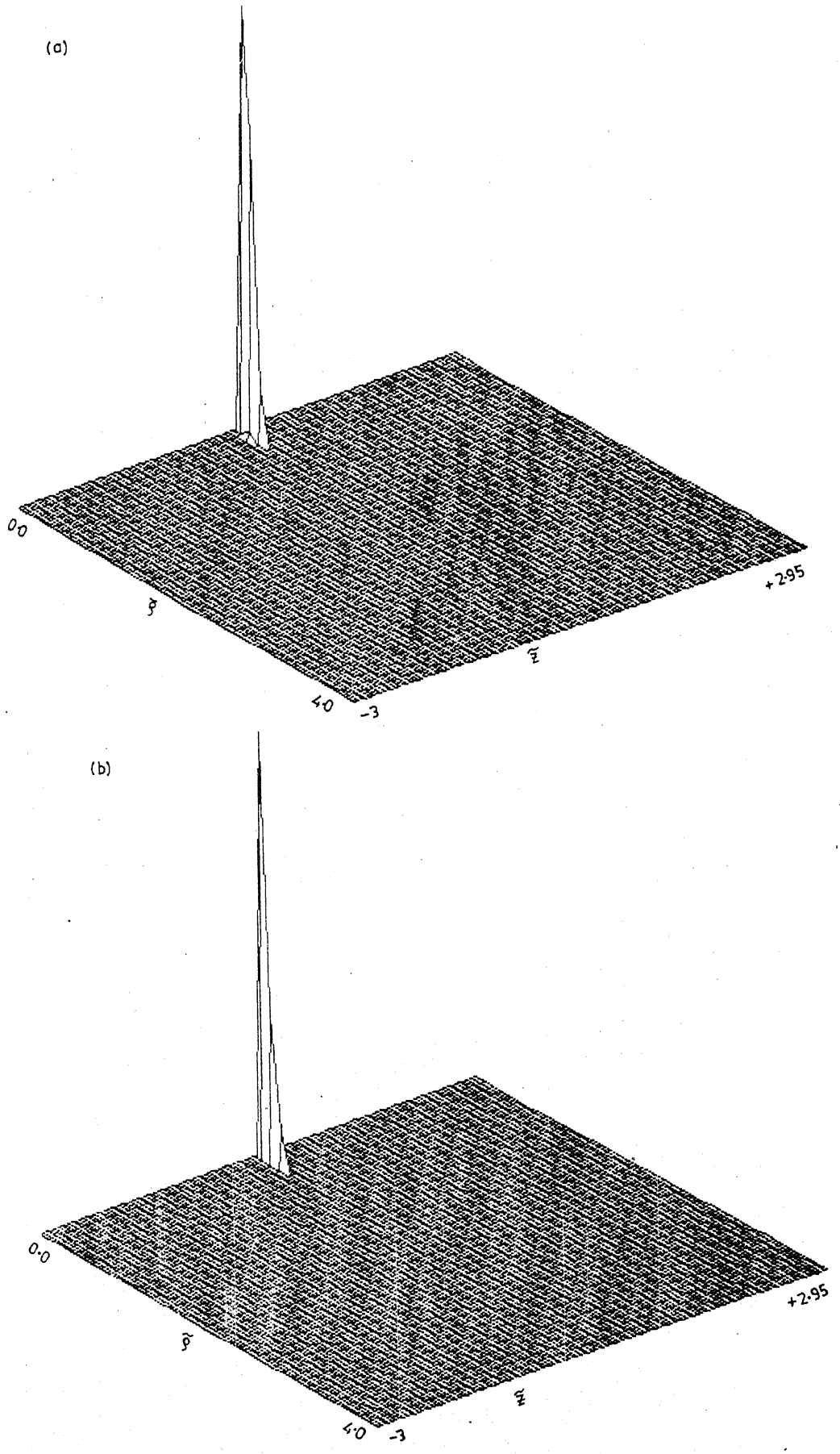

Figure 3. Perspective plots (a.u.) of current density ($|\mathbf{j}|$) of nitrogen atom colliding with a proton in cylindrical polar coordinates ($\tilde{\rho}, \tilde{z}$). See caption of figure 1 for details. $t = 5{\cdot}0$ (**a**), $15{\cdot}0$ (**b**).

does not show much change in contrast to the conspicuous change in v_{eff} plot at that time step. Accumulation of charge density near the origin is due to self modulation (Hasegawa 1975), a typical nonlinear effect. This effect is not an artifact of the QFDF formalism because it has been shown (Takabayashi 1983) that the GNLSE (12) will not show any unphysical nonlinear behavior if dynamics is not actually nonlinear.

Figures 3a and b depict the time evolution of $|\mathbf{j}|$ at $t = 5$ and 15 (in a.u.) respectively. These plots are similar to those of charge density at those time steps. In each of the figures current density shows a maximum at the nuclear site where ρ is also high. The nonvanishing current density at nonzero time indicates that the excited states of the nitrogen atom are getting mixed with its ground state as the proton approaches it.

Spatial profiles of $-\nabla^2\rho$ at $t = 0, 5, 15$ (in a.u.) are shown in figures 4a–c respectively. The vertical dimensions of these plots are taken between -10 and $+10$. Initially, at $t = 0$ (figure 4a), $-\nabla^2\rho$ shows two maxima and one minimum as was observed by Bader *et al* (1984). The first maximum around $\tilde{z} = 0$ corresponds to the core region and outer minimum and maximum are formed due to the valence shell. It may be noted that the signature of this shell–structure is also present in the v_{eff} plot at this time step. Trough and crest in v_{eff} correspond respectively to charge accumulation and depletion which in turn are related to maximum and minimum in $-\nabla^2\rho$, a fact in conformity with Bader's observation (Bader *et al* 1984). The radius of the nitrogen atom is calculated as the average distance where charge accumulation of the valence shell is maximum (which corresponds to the second maximum in the $-\nabla^2\rho$ plot). It was found to be 0·414 Å which is close to Bader's value of 0·411 Å (Bader *et al* 1984). At later time steps, the ground state shell structure of the nitrogen atom is lost as $-\nabla^2\rho$ plots in figures 4b and c consists of one high peak at the high density region and one trough. The shrinking of the base of the high peak in $-\nabla^2\rho$ plot indicates the accumulation of density at the nuclear site.

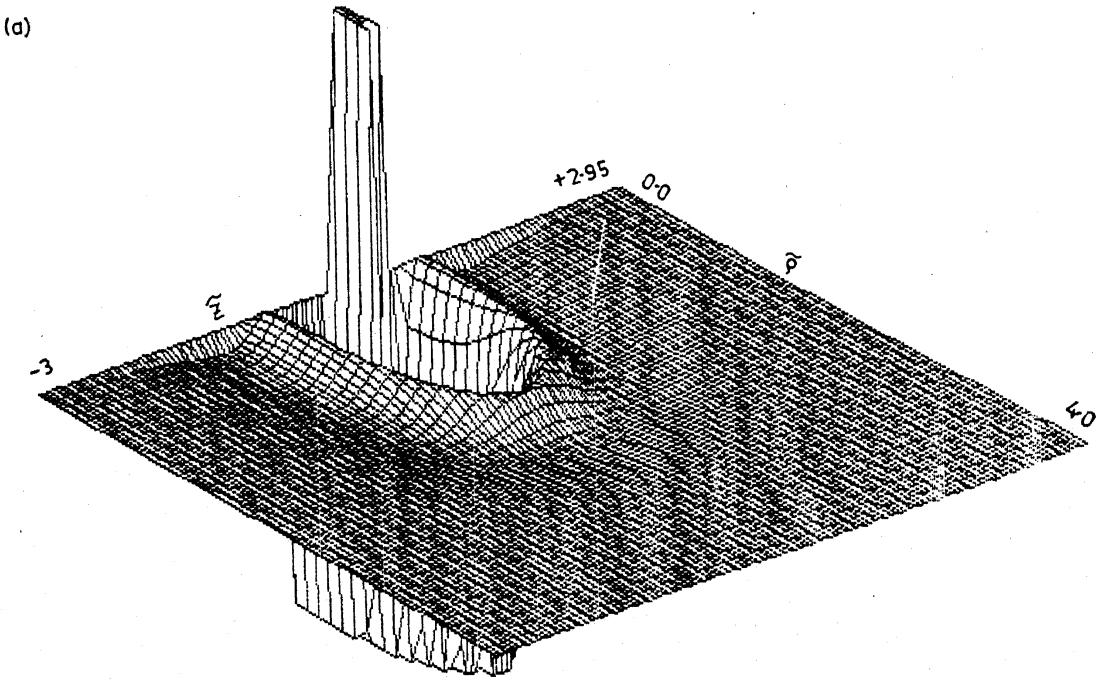

Figure 4. (a) (Caption on facing page.)

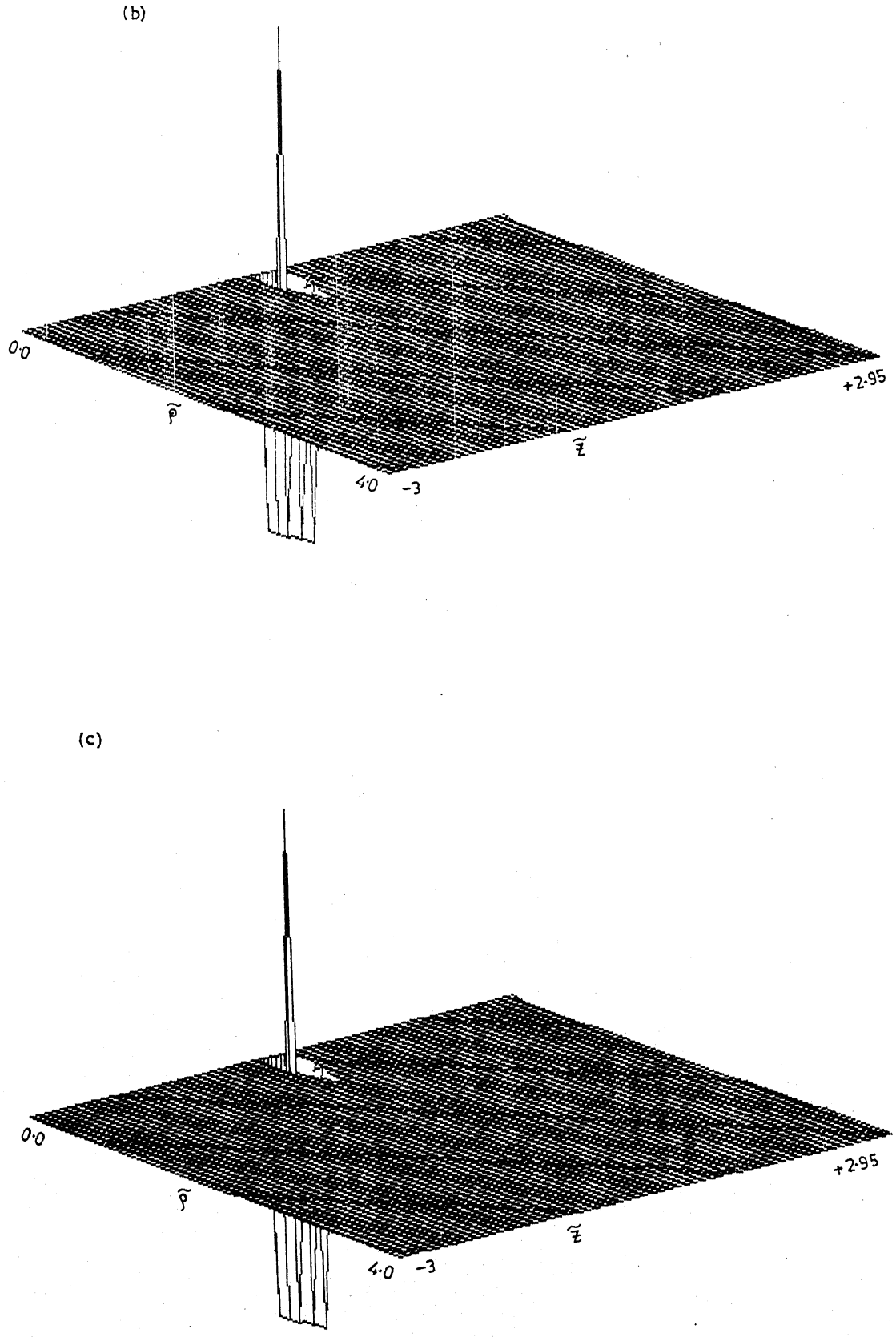

Figure 4. Perspective plots (a.u.) of $-\nabla^2\rho$ of nitrogen atom colliding with a proton in cylindrical polar coordinates $(\tilde{\rho}, \tilde{z})$. See caption of figure 1 for details. $t = 0{\cdot}0$ (**a**), $5{\cdot}0$ (**b**), $15{\cdot}0$ (**c**).

Plot of $\eta(\mathbf{r})$ at $t = 0$, shows a high peak at the high density region (figure 5a). Some small undulations have been found along the increasing $\tilde{\rho}$ axis, around $\tilde{z} = 0$ which gets magnified in later time steps (figures 5b and c). The peak position of $\eta(\mathbf{r})$ at later time steps remains unaltered though the base of the peak shrinks as density gets concentrated around the nitrogen nucleus.

The presence of a high peak of $\eta(\mathbf{r})$ at the high density region agrees well with the fact that hard–hard interactions are charge-controlled (Klopman 1974). It is also found by Lee *et al* (1988) from *ab initio* MO calculations that in linkage isomers SCN^-, the nitrogen end possessing maximum gross charge is harder. In the present case, $\eta(\mathbf{r})$ plots resemble density plots more than $-\nabla^2\rho$ plots.

The plot of entropy density $s(\mathbf{r}, t)$ at $t = 0$ (figure 6a) shows a high peak around $\tilde{\rho} = 0, \tilde{z} = 0$. This peak and a nearby trough are surrounded by a ridge-like structure. In later time steps (figures 6b and c) the trough and the ridge-like structure disappear. Only one peak is found at the high density region. The maximum entropy zone, associated with a high value of probability density, is a consequence of MEP (Jaynes 1963).

Figures 7a and b depict the surprisal plots at $t = 5$ and 15 (in a.u.) respectively. In both figures, I shows a deep trough where ρ is high. The trough is surrounded by a ridge-like structure. There is not much difference between I plots at $t = 5$ and $t = 15$

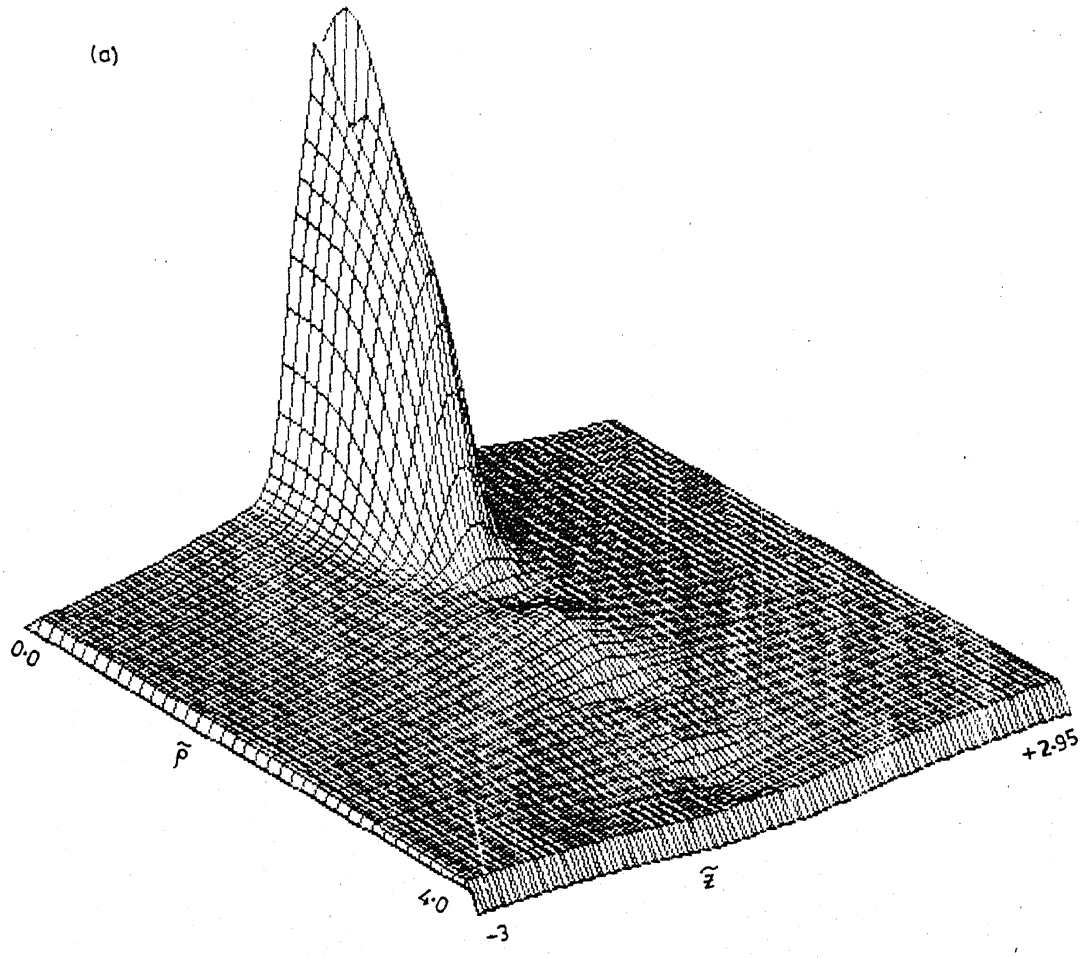

Figure 5. (a) (Caption on facing page.)

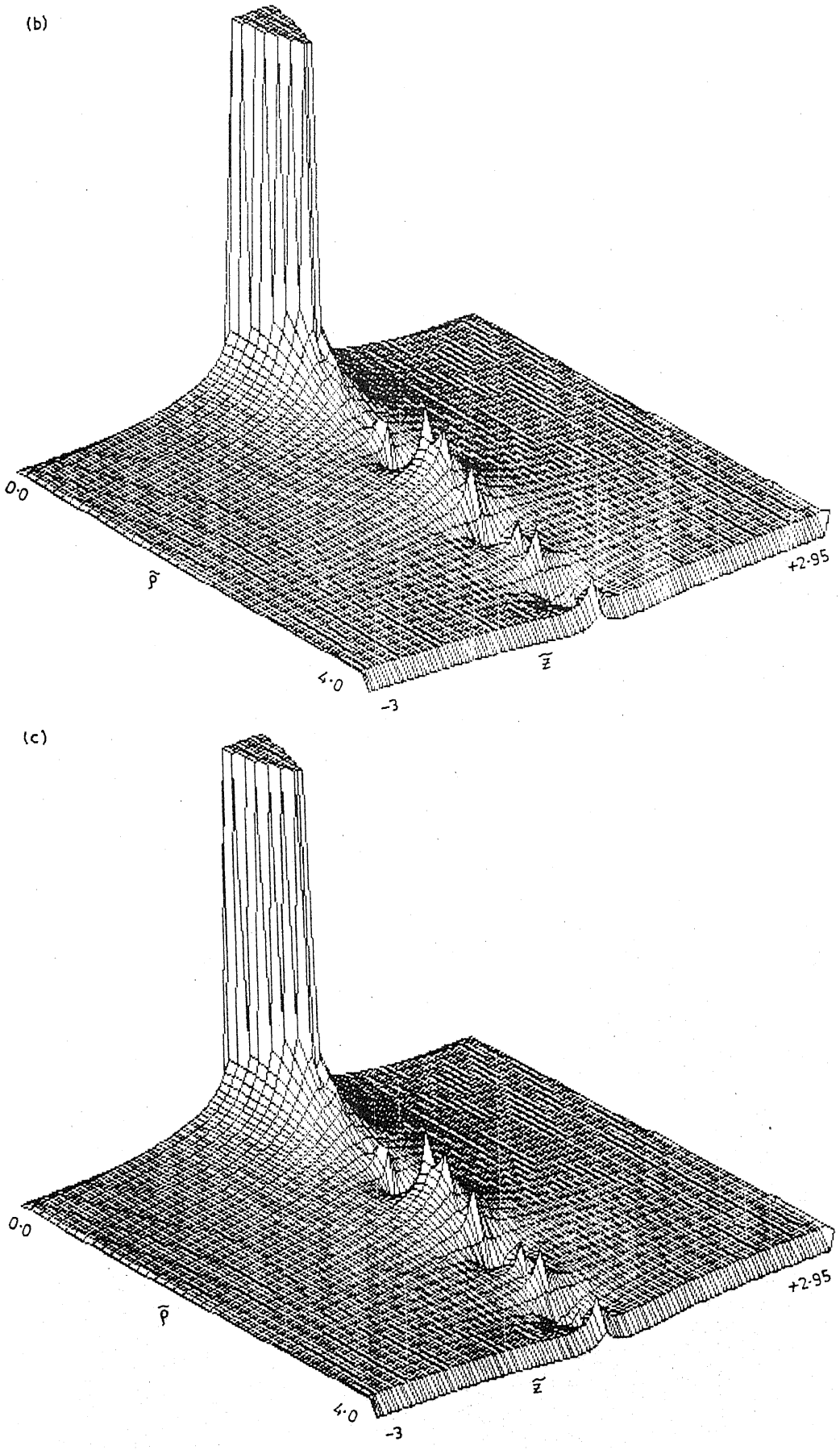

Figure 5. Perspective plots (a.u.) of local hardness ($\eta(\mathbf{r})$) of nitrogen atom colliding with a proton in cylindrical polar coordinates ($\tilde{\rho}, \tilde{z}$). See caption of figure 1 for details. $t = 0{\cdot}0$ **(a)**, 5·0 **(b)**, 15·0 **(c)**.

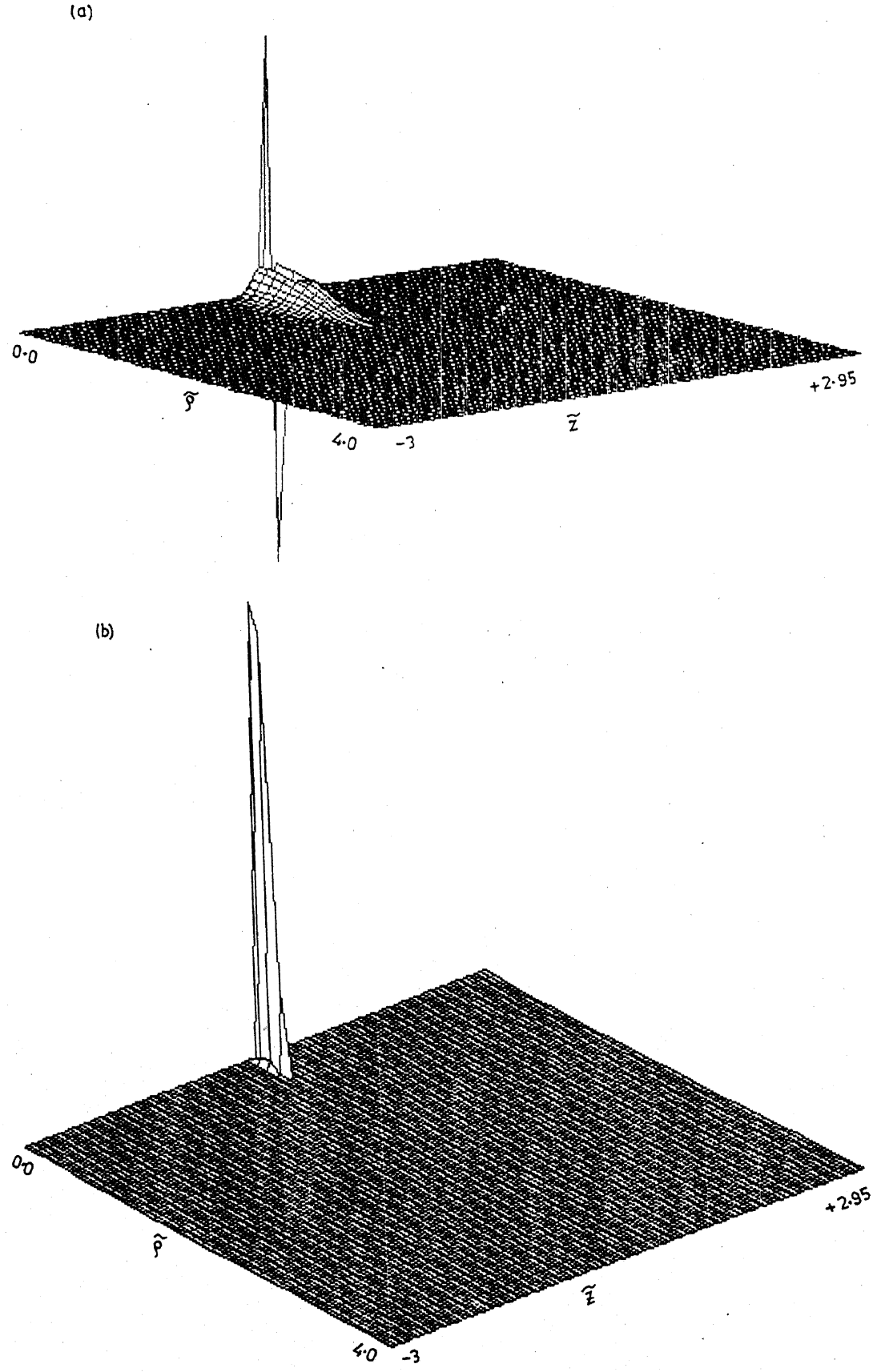

Fiugre 6. (**a**) & (**b**) (Caption on facing page.)

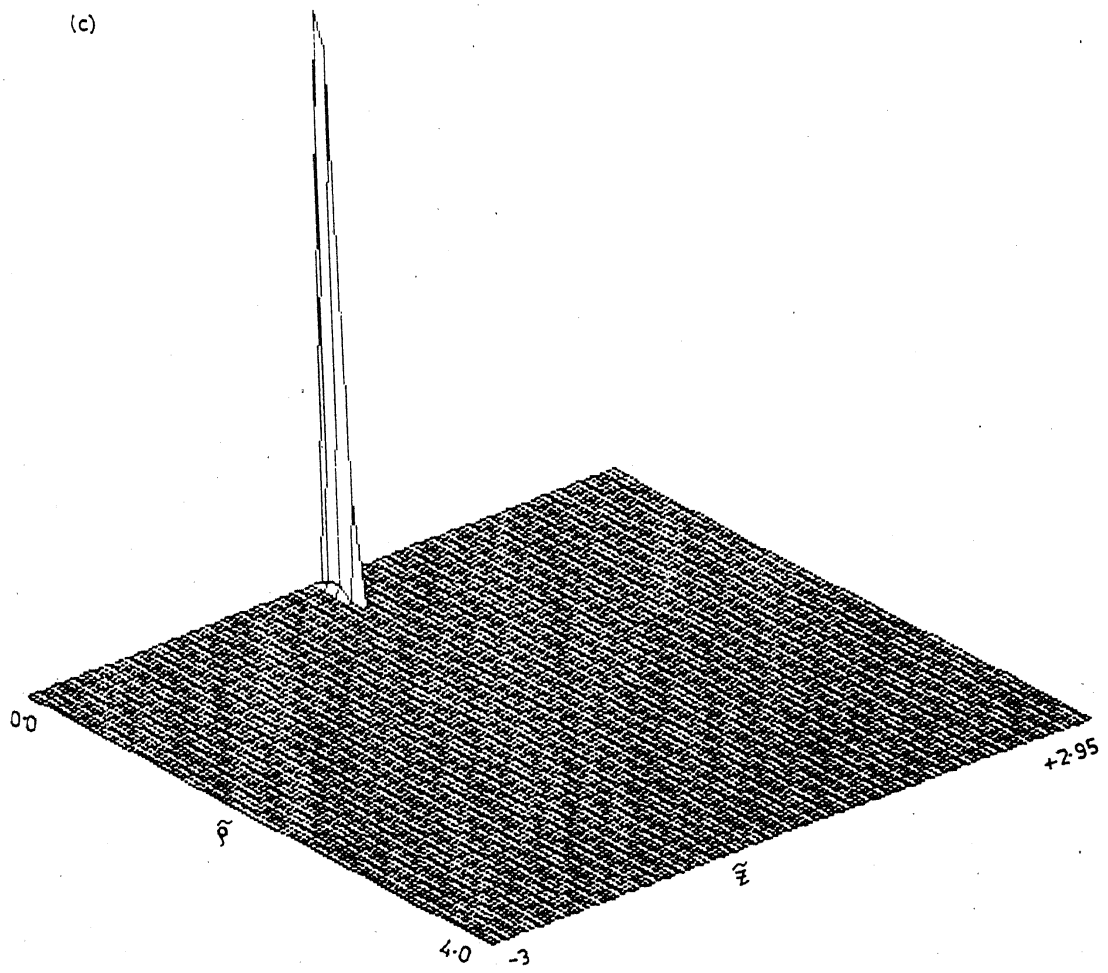

Figure 6. Perspective plots (a.u.) of entropy density ($s(\mathbf{r}, t)$) of nitrogen atom colliding with a proton in cylindrical polar coordinates ($\tilde{\rho}, \tilde{z}$). See caption of figure 1 for details. $t = 0{\cdot}0$ (**a**), 5·0 (**b**), 15·0 (**c**).

(in a.u.) which indicates that the process of NH^+ supermolecule formation has reached a situation where further change in time-dependent profiles is not conspicuous.

Temporal evolution of η is presented in figure 8. Global hardness is found to increase with time and to ultimately reach a high value. It remains constant thereafter. As there is a negligible change in density and surprisal plots after certain time steps, it seems that the whole system of NH^+ supermolecule has reached some sort of "dynamic equilibrium". So the maximisation of global hardness in a dynamical process may be thought of as a consequence of the maximum hardness principle (Pearson 1987; Parr and Chattaraj 1991) in a time-dependent situation.

Time evolution of global hardness, does not enable one to divide the scattering process in three regimes, namely, approach, encounter and departure corresponding to approach, interaction and departure of proton as has been possible in case of time evolution of μ (Chattaraj and Nath 1994a). However, time evolution of entropy (S) presented in figure 9, shows that in the interaction regime entropy increases to a maximum value and then decreases indicating the formation of a stable NH^+ species. A preliminary report of this work is given in Chattaraj and Nath (1994b).

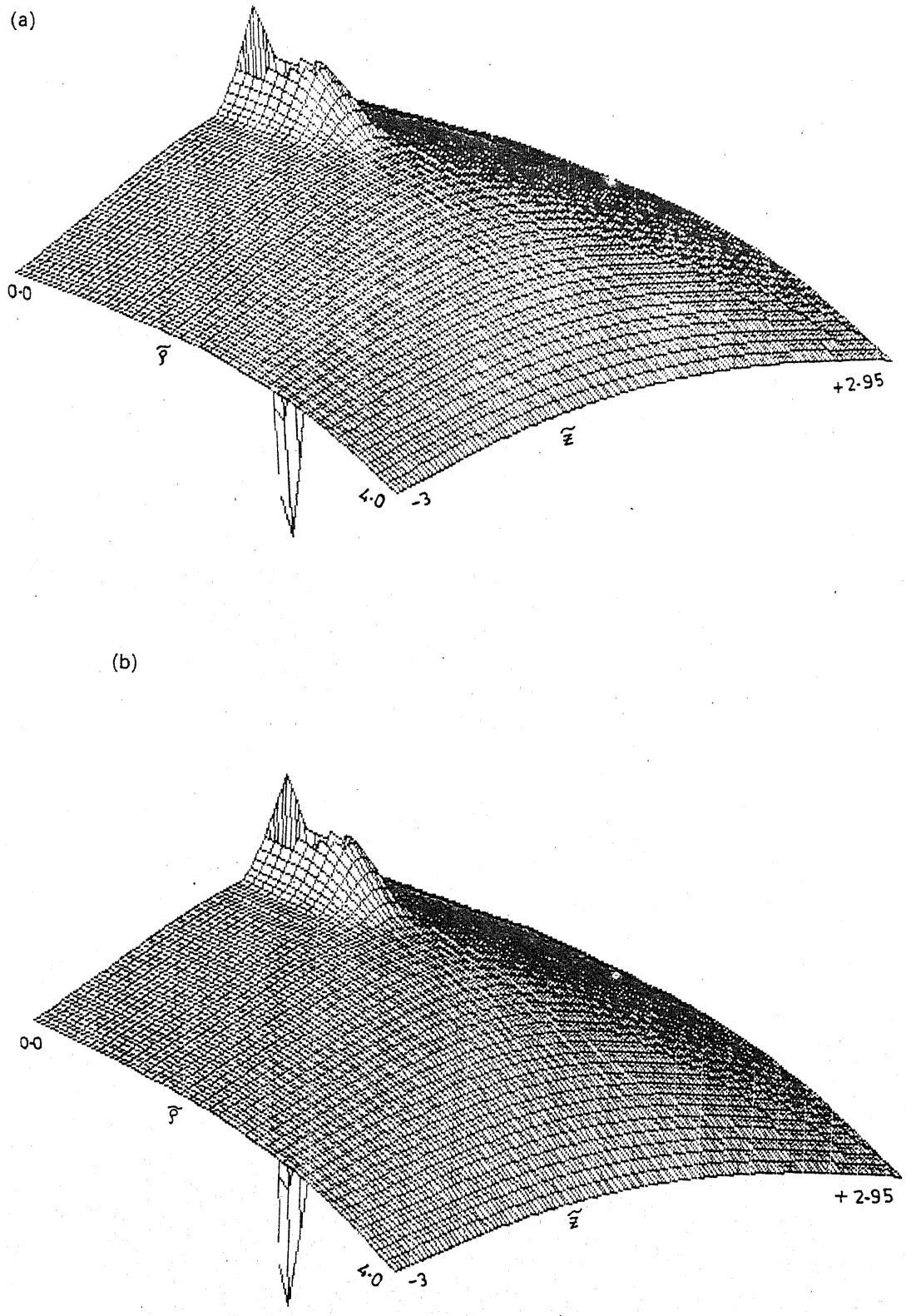

Figure 7. Perspective plots (a.u.) of surprisal(I) of nitrogen atom colliding with a proton in cylindrical polar coordinates ($\tilde{\rho}$, $\tilde{z}$). See caption of figure 1 for details. $t = 5{\cdot}0$ **(a)**, $15{\cdot}0$ **(b)**.

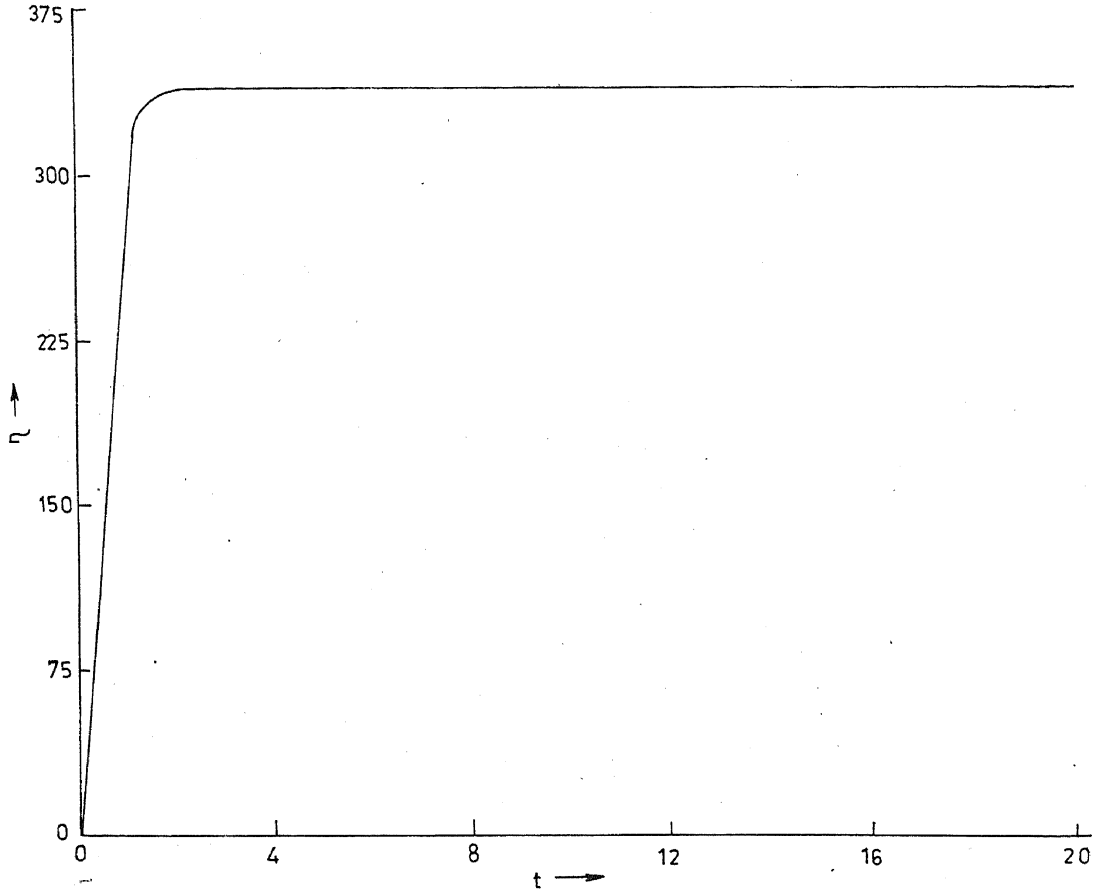

Figure 8. Time dependence of global hardness (η) of nitrogen atom colliding with a proton.

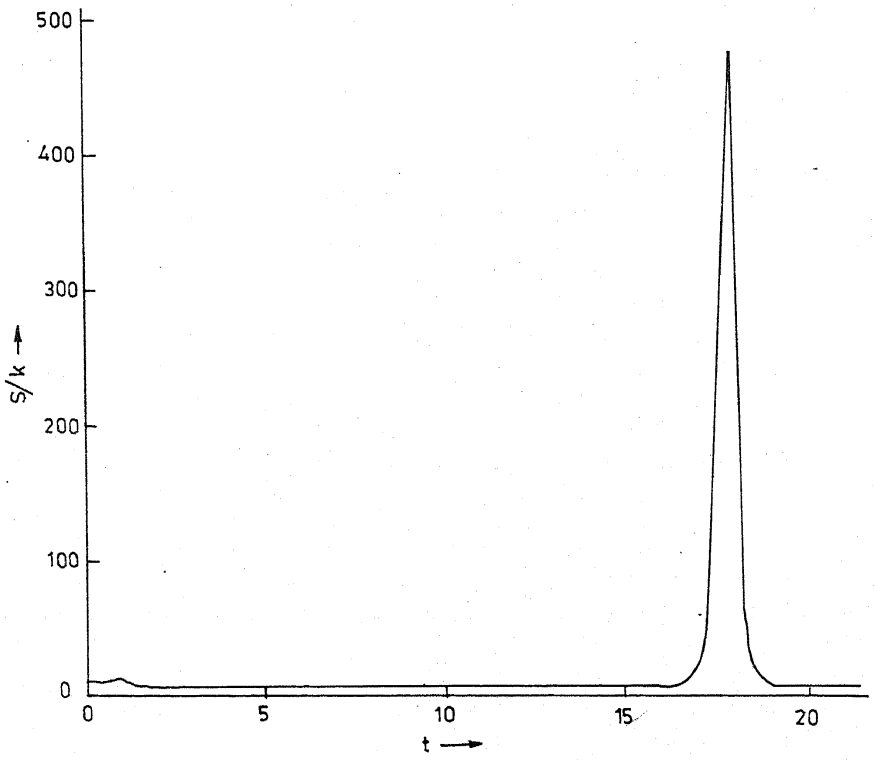

Figure 9. Time dependence of entropy (S) of nitrogen atom colliding with a proton.

4. Conclusion

In the present work, values of local and global hardnesses of a nitrogen atom in a field created by an approaching proton have been computed and the dynamics of global and local hardnesses have been studied for the first time within a quantum fluid density functional framework. Evolution of global hardness to a maximum value may be treated as the dynamical extension of the maximum hardness principle. An approximate functional form for $f(\mathbf{r})$ has been presented and the direction towards its improvement has been discussed. Increase of entropy in the interaction regime indicates that the reaction of a proton with the nitrogen atom to form NH^+ is a favourable process. Maximisation of entropy during the interaction between H^+ and nitrogen atom is a consequence of the maximum entropy principle. In this study it has not been possible to characterise the state of the NH^+ molecule if at all it has been produced. Further study in this direction especially in predicting, from the maximum hardness principle, in which state the NH^+ molecule is formed would be important.

Acknowledgements

PKC would like to thank CSIR, New Delhi for financial assistance.

References

Bader R F W, Mac Dougall P J and Lau C D H 1984 *J. Am. Chem. Soc.* **106** 1594
Baeck K K and Lee Y S 1990 *J. Chem. Phys.* **93** 5775
Berkowitz M, Ghosh S K and Parr R G 1985 *J. Am. Chem. Soc.* **107** 6811
Chattaraj P K 1992a *Int. J. Quant. Chem.* **41** 845
Chattaraj P K 1992b *J. Indian Chem. Soc.* **69** 173
Chattaraj P K and Nath S 1994a *Int. J. Quant. Chem.* (in press)
Chattaraj P K and Nath S 1994b *Chem. Phys. Lett.* **217** 342
Chattaraj P K, Nath S and Sannigrahi A B 1993 *Chem. Phys. Lett.* (in press)
Chattaraj P K and Parr R G 1993 In *Chemical hardness, Structure and bonding, Vol. 80* (eds) K D Sen and D M P Mingos (Berlin: Springer) pp. 11–26
Chattaraj P K and Schleyer P v R 1994 *J. Am. Chem. Soc.* **116** 1067
Clementi E and Roetti C R 1974 *At. Data Nucl. Data Tables* **14** 174
Colin R and Douglas A E 1968 *Can. J. Phys.* **46** 61
Dal Pino A Jr, Galvan M, Arias T A and Joannopoulos J D 1993 *J. Chem. Phys.* **98** 1606
Datta D 1992a *Inorg. Chem.* **31** 2797
Datta D 1992b *J. Phys. Chem.* **96** 2409
Deb B M and Chattaraj P K 1988 *Chem. Phys. Lett.* **148** 550
Deb B M and Chattaraj P K 1989 *Phys. Rev.* **A39** 1696
Deb B M, Chattaraj P K and Mishra S 1991 *Phys. Rev.* **A43** 1248
Dhara A K and Ghosh S K 1987 *Phys. Rev.* **A35** 442
Gadre S R and Bendale R D 1985 *Curr. Sci.* **54** 970
Galvan M, Dal Pino A Jr and Joannopoulos J D 1993 *Phys. Rev. Lett.* **70** 21
Gazquez J L 1993 In *Chemical hardness, Structure and bonding, Vol. 80* (eds) K D Sen and D M P Mingos (Berlin: Springer)
Ghosh S K and Balbas L C 1985 *J. Chem. Phys.* **83** 5778
Ghosh S K and Berkowitz M 1985 *Chem. Phys.* **83** 2976
Harbola M K 1992 *Proc. Natl. Acad. Sci. USA* **89** 1036

Harbola M K, Chattaraj P K and Parr R G 1991 *Isr. J. Chem.* **31** 395
Hasegawa A 1975 *Plasma instability and nonlinear effects* (Berlin: Springer–Verlag)
Hati S and Datta D 1992 *J. Org. Chem.* **57** 6056
Hohenberg P and Kohn W 1964 *Phys. Rev.* **B136** 864
Huber K P and Herzberg G 1979 *Molecular spectra and molecular structure. IV. Constants of diatomic molecule* (New York: Van Nostrand–Reinhold) p. 460
Jaynes E T 1963 In *Statistical physics. Vol. 3. Brandeis Lectures* (ed.) K W Ford (New York: Benjamin)
Klopman G (ed.) 1974 In *Chemical reactivity and reaction path* (New York: Wiley) chap. 4
Lee C, Yang W and Parr R G 1988 *J. Mol. Struc. (Theochem.)* **163** 305
Levine R D and Bernstein R B 1976 In *Dynamics of molecular collisions* (ed.) W H Miller (New York: Plenum)
Liu H P D and Verhaegen 1970 *J. Chem. Phys.* **53** 735
Nath S, Sannigrahi A B and Chattaraj P K 1994a *J. Mol. Struct. (Theochem.)* **306** 87
Nath S, Sannigrahi A B and Chattaraj P K 1994b *J. Mol. Struct. (Theochem.)* (in press)
Parr R G and Chattaraj P K 1991 *J. Am. Chem. Soc.* **113** 1854
Parr R G, Donnelly R A, Levy M and Palke W E 1978 *J. Chem. Phys.* **68** 3801
Parr R G and Gazquez J L 1993 *J. Phys. Chem.* **97** 3939
Parr R G and Pearson R G 1983 *J. Am. Chem. Soc.* **105** 7512
Parr R G and Yang W 1982 *J. Am. Chem. Soc.* **104** 3801
Parr R G and Yang W 1989 *Density functional theory of atoms and molecules* (New York: Oxford)
Pearson R G 1987 *J. Chem. Educ.* **64** 561
Pearson R G 1988 *Inorg. Chem.* **27** 734
Pearson R G 1990 In *Theoretical models of chemical bonding. Part II* (ed.) Z B Maksic (Berlin: Springer–Verlag) pp. 45–76
Pearson R G and Palke W E 1992 *J. Phys. Chem.* **96** 3283
Runge E and Gross E K U 1984 *Phys. Rev. Lett.* **52** 997
Sen K D and Jorgensen C K (eds) 1987 *Electronegativity. Structure and bonding. Vol. 66* (Berlin: Springer–Verlag)
Sen K D and Mingos D M P (eds) 1993 *Chemical hardness. Structure and bonding. Vol.* 66 (Berlin: Springer)
Takabayashi T 1983 *Prog. Theor. Phys. Jpn.* **69** 1323
Yang W and Parr R G 1985 *Proc. Natl. Acad. Sci. USA* **82** 6723
Zhou Z and Parr R G 1989 *J. Am. Chem. Soc.* **111** 7371
Zhou Z and Parr R G 1990 *J. Am. Chem. Soc.* **112** 5720
Zhou Z, Parr R G and Garst J F 1988 *Tetrahedron Lett.* **29** 4843